Real-Time Driving Risk Assessment Using LSTM-attention and XGBoost with Physiological and Driving Behavior Data

Real-Time Driving Risk Assessment Using LSTM-attention and XGBoost with Physiological and Driving Behavior Data

Yecan Wang[1], Michele Guagnano[2,4], Hiroki Taniguchi[1], Nozomi Nagatani[1], Hiroshi Ono[1], Satoru Shinkawa[1], Sumie Miyamoto[3], Eriko Hasumi[3], Katsuhito Fujiu[3], Madoka Takai[3], Massimo Violante[2], Shigenobu Mitsuzawa[1]

Abstract— **Early identification of driving risks is crucial for driving safety. In this study, a deep learning method based on Long Short-term Memory (LSTM) with attention mechanism and XGBoost to recognize risk levels during driving simulation for early warnings, has been proposed. Here, we collected multimodal data -including driving data, eyes status, and basic physiological data-from driving simulators, eye trackers, and smartwatches for comprehensive analysis. By combining driving behavior and physiological features in each time window, the ability of LSTM networks was applied to analyze temporal features for prediction of the risk levels (Level 0, Level 1, and Level 2) in the next 20 seconds. Meanwhile, an attention mechanism was introduced to understand the importance of multiple features as well. Then the output of LSTM-attention was further refined using XGBoost, which demonstrated excellent performance in classification tasks. The integrated model showed that the overall accuracy achieved is above 89.97%, with an F1-score of 89.15%.**

I. INTRODUCTION

Traffic accidents have become a major global public safety issue, resulting in over 1.3 million fatalities annually [1]. Among the reported accidents, approximately 90% are attributed to risky driving behaviors and improper operations, leading to substantial and often immeasurable economic losses [2]. The interplay of various human factors- including alcohol consumption, fatigue, distraction, and speeding-further exacerbates driving risks [3][4][5]. Therefore, real-time monitoring of driving conditions, early identification of risk, and timely safety warnings are crucial for enhancing traffic safety. Currently, Advanced Driver Assistance Systems (ADAS), which can detect or predict various potential collisions by integrating information about hazardous conditions in the traffic environment, have been widely deployed to help timely alerts imminent risks as early as possible [6]. However, the existing detection mechanisms remain primarily focused on external factors driven by vehicle dynamics and surrounding environments, while neglecting the interaction with the driver's state, leading to significant limitations on the accuracy of risk prediction.

With the rapid development of technologies such as in-vehicle sensors and wearable devices, an increasing number of studies have begun to utilize multimodal driving data in combination with machine learning and deep learning algorithms to assess and predict driving risk [7]. Guo et al. stated a traffic crash prediction model, based on random forest and logistic regression, integrating risky driving behavior and traffic flow data [8]. With the key factors of traffic volume, speed, congestion index, and abrupt acceleration, the nonlinear interactions between traffic flow and driving behaviors was revealed, and the effectiveness in real-time crash risk assessment was demonstrated with the accuracy of 84.48% and false alarm of 9.75%. In addition, driving behavior characteristics are inherently time-series data, and driving risk on roads exhibits temporal dependency [9]. Zhang et al. studied a method to identify high risky drivers using short period driving data by analyzing temporal variations in driving behavior instead of traditional aggregated statistics [10]. Leveraging CNN and LSTM models along with a novel "traffic entropy" index, the approach improved prediction accuracy and supported more effective safety management.

Although hybrid models decrease the predominant reliance on single-model approaches and mitigate model-specific limitations, the inherent complexity not only elevates overfitting risks but also diminishes interpretability. In addition, in real-world driving scenarios, vehicles predominantly operate in safe states during most driving scenes, leading to uneven data distribution where low-risk instances dominate. This imbalance adversely impacts model performance in accurately evaluating rare-class samples.

In this study, we introduced a hybrid early risk prediction model based on Long Short-term Memory (LSTM) and XGBoost, integrating driving status, basic physiological data, and road type to predict short-term driving risk in real time. The multimodal data were collected by driving simulator, eye-tracker, and smartwatch. Combining Eboli et al.'s work [11], features were engineered by LSTM with attention mechanism and fine-tuned using XGBoost to improve performance. The contributions of this study are as follows:

- We introduce a hybrid LSTM-attention-XGBoost model to enhance the real-time prediction ability of driving behaviors, the performance of which is more excellent compared with classic methodologies.
- Hierarchical processing strategies, exemplified by XGBoost fine-tuning of LSTM outputs, effectively

*Research supported by Honda Motor R&D Co., Ltd. The experiment was approved by ethic review committees from Honda Motor R&D (No.100HM-021H) and University of Tokyo (No. 2023238NI).

[1]Yecan Wang, Hiroki Taniguchi, Nozomi Nagatani, Hiroshi Ono, Satoru Shinkawa, and Shigenobu Mitsuzawa are with Honda Motor R&D Co., Ltd.,Wako, 351-0113, Saitama, Japan (corresponding author to provide phone: 080-4949-2650; e-mail: shingenobu_mitsuzawa@ jp.honda).

[2]Michele Guagnano and Massimo Violante are with Politecnico di Torino, Dip. Automatica e Informatica, Italy and Sleep Advice Technologies, Torino, Italy (e-mail: massimo.violante@polito.it).

[3]Sumie Miyamoto, Eriko Hasumi, and Katsuhito Fujiu, are with the Department of Medical. Madoka Takai is with the Department of Bioengineering, the University of Tokyo, 113-8654, Tokyo, Japan (e-mail: takai@bis.t.u-tokyo.ac.jp)

mitigate bias toward majority classes caused by data imbalance. This approach prevented secondary data processing techniques, such as synthetic minority over-sampling technique (SMOTE), while optimizing classification performance.

- Integration of attention mechanisms enables the capture of factors weights in driving risk assessment, thereby enhancing interpretability of the model and providing insights into feature contributions.

The rest of the paper is organized as follows. Section II presents the methodology we developed, Section III to V presents the experiments we performed, and discuss the results we achieved and the limitations we found. Finally, Section VI draws some conclusions.

II. METHODOLOGY

This section introduces a hybrid approach designed for real-time prediction of hazardous driving behaviors. The methodology initiates with a safety classification protocol, where the driving status are binary categorized at each temporal data point based on kinematic parameters, followed by a hierarchical risk grading system according to the proportion of unsafe driving within one second. Afterwards, the sequential safety status occurred in a certain period are processed by LSTM-attention due to its capacity of modeling temporal dependencies in time-series data. Then the preliminary LSTM predictions are refined by XGBoost to optimize the minority-class discrimination.

A. Identification of driving behavior

Acceleration and velocity are commonly regarded as the principal parameters employed in the analysis of driving behaviors [12][13]. Referring to Eboli and co-authors' work [11], this study adapted conservative assumptions, including a constant friction coefficient and no superelevation in curves, to investigate the acceleration vector of vehicle in a circle curve where the resultant force (F_R) is balanced by the side friction (μ) and vehicle mass (m) as (1). Three driving conditions were defined: safe ($F_S < F_R$), limit ($F_S = F_R$), and unsafe ($F_S > F_R$), where Fs was the stimulate force obtained by the second law of Newton, shown as (2).

$$F_R = m * g * \mu \quad (1)$$

$$F_S = m * \sqrt{a_x^2 + a_y^2} \quad (2)$$

Where a_x and a_y represented accelerations in lateral and longitudinal directions, respectively. This methodology approximates the ellipse of adherence with a circle to simplify calculations, resulting in a quadratic relationship between acceleration and speed (V), expressed as (3).

$$\sqrt{a_x^2 + a_y^2} = g * \left[0.198\left(\frac{V}{100}^2\right) - 0.592\left(\frac{V}{100}\right) + 0.569\right] \quad (3)$$

According to the formula, safe driving conditions were within the defined limits, while unsafe ones exceeded them. This method provided one clear and visual protocol to classify the driving behavior in each recording moment. Due to the interval resolution of 10 milliseconds in the driving simulator, the safety assessment of driving behavior per second will be quantified by the proportion of unsafe driving behaviors within each one-second period.

B. LSTM with attention mechanism

LSTM, as a special type of recurrent neural network (RNN), is commonly used to address the issues of vanishing or exploding gradients, enabling the learning of long-term

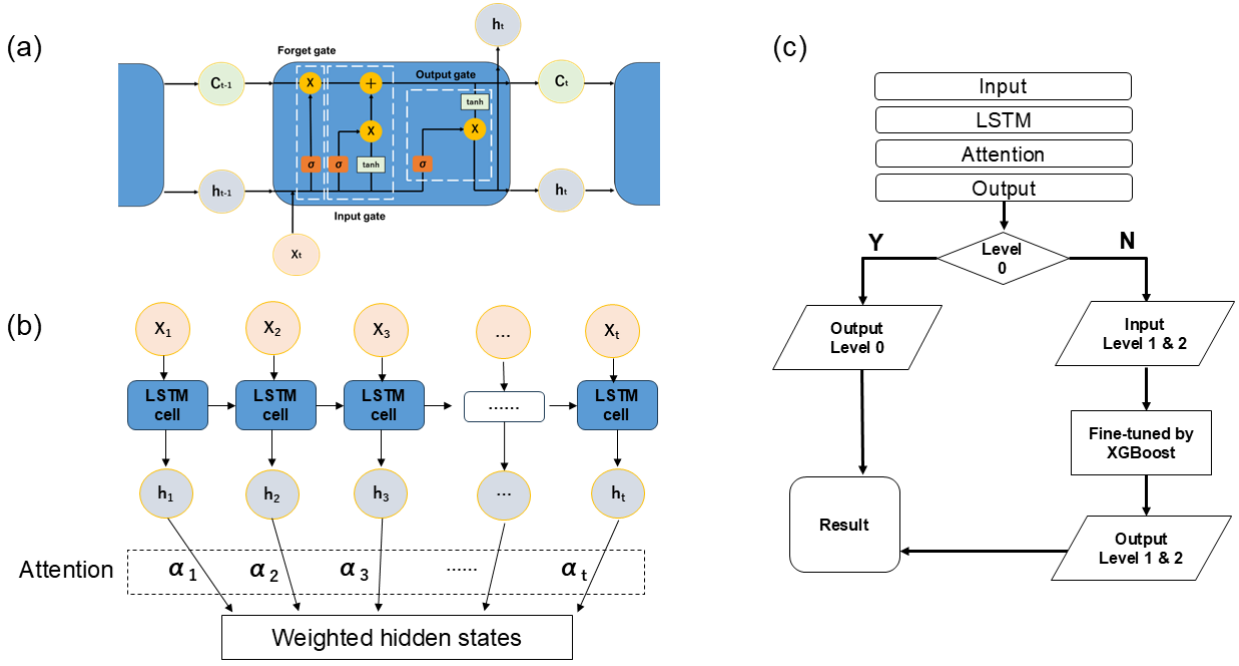

Fig 1. (a) The structure of LSTM cell. (b) The model of LSTM with attention. (c) The flowchart of LSTM-attention model with XGBoost.

dependencies. As illustrated in Fig 1(a), an LSTM unit consists of a cell state and three gates: the input gate determining which new information to add, the forget gate deciding which information to discard from the cell state, and the output gate controlling which information to output. Detailed descriptions of each LSTM cell are provided in Equations (4), (5), and (6), while the final cell state and hidden state of each unit can be represented by Equations (7) and (8), respectively.

$$f_t = \sigma(W_f \begin{bmatrix} h_{t-1} \\ x_t \end{bmatrix} + b_f) \tag{4}$$

$$i_t = \sigma(W_i \begin{bmatrix} h_{t-1} \\ x_t \end{bmatrix} + b_i) \tag{5}$$

$$o_t = \sigma(W_o \begin{bmatrix} h_{t-1} \\ x_t \end{bmatrix} + b_o) \tag{6}$$

$$C_t = f_t C_{t-1} + i_t \tanh(W_c \begin{bmatrix} h_{t-1} \\ x_t \end{bmatrix} + b_c) \tag{7}$$

$$h_t = o_t \tanh(C_t) \tag{8}$$

Where f_t, i_t, and o_t correspond to the forget gate, input gate, and output gate, respectively. h_t denotes the hidden state, and C_t represents the cell state of the LSTM unit. σ denotes the sigmoid function. The term b and W indicate the offset and weight indicator, respectively. According to the multiple features, the LSTM model outputs a driving risk level of 'Level 0', 'Level 1', and 'Level 2', representing 'Safe', 'Normal', and 'Unsafe', respectively.

At the same time, an attention layer was introduced, which selected features for time series data through global feature weights, enhancing the sensitivity to key features, and provided an intuitive explanation of feature importance (Fig 1(b)). The architecture of attention layer is explicitly defined in Equations (9) and (10).

$$\alpha_t = softmax(\tanh(W_h h_t + b_h)) \tag{9}$$

$$Weighted\ hidden\ states = \sum_N \alpha_t h_t \tag{10}$$

Where α represents an attention weight vector. Therefore, attention mechanism balances computational efficiency and interpretability.

C. XGBoost

XGBoost is a decision tree-based deep learning algorithm widely used for its efficiency and superior performance in classification tasks. This model incorporates regularization techniques to prevent overfitting, ensuring robust generalization to invisible data. The ability to customize loss functions and evaluation metrics enables us to adapt to various scenarios. In this study, the categories with lower accuracy obtained by the LSTM-attention were used as input and fine-tuned with XGBoost to improve the overall performance of the model via gradient-boosted decision trees. The flowchart of the hybrid model was shown in Fig 1(c).

III. EXPERIMENT

A. Experiment design

In collaboration with the University of Tokyo, we installed four driving simulators and recruited 54 volunteers (28 males and 26 females), with a mean age of 44.6±15.5 years ranging from 20 to 65 years old, to participate in the research. Each volunteer chose their testing times among 10:30 AM, 13:30 PM, 15:30 PM, and 17:30 PM on weekdays over a six-month period, completing 12 sessions (the first being a practice session) in total. During each session, volunteers were required to complete a planned scenario four times within one hour, including one segment of detour (Fig 2(a)). Meanwhile, volunteers wore Garmin smartwatches to record physiological data such as heart rate and heart rate variability. Additionally, Tobii Pro eye trackers recorded participants' eye movements. Between all testing sessions, volunteers underwent cognitive tests to ensure no cognitive impairments.

B. Data processing

Due to technical issues and unforeseen circumstances, some physiological data and driving data were incomplete. To ensure data integrity, volunteers' records with more than 20% missing data were excluded and prioritized those with complete recorded dataset were selected as priority. After data cleaning and supplementation, we referred to Eboli et al.'s work [11] to determine whether a recorded moment was safe based on instantaneous speed and acceleration. Fig 2(b) shows the distribution of driving behaviors for two volunteers during one lap of scenario, where green and orange represented safe behavior and unsafe behavior, respectively.

Main features are shown in Table I. Speed and acceleration had been established as vital parameters for characterizing safe and unsafe driving behaviors. Consequently, the prediction model incorporated the mean and standard deviation of yaw angle, combining with the mean and standard deviation of steering wheel steering angle, as driving features. The wheel steering angle and yaw angle were both

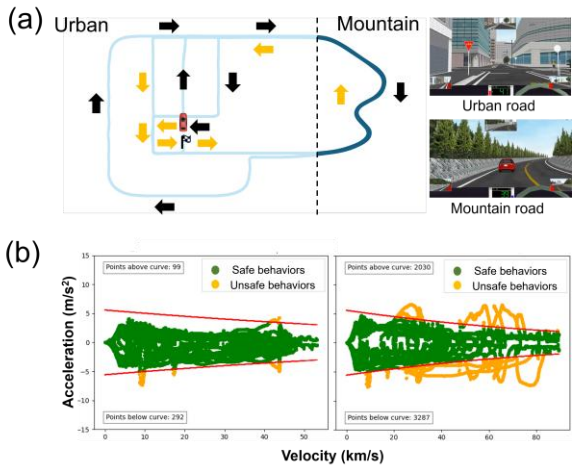

Fig 2. (a) The route map with urban road and mountain road set in the driving simulator, where black arrows and yellow arrows represent the orientations of the first and second circles in one lap, respectively. (b) Examples of classification results of driving behaviors (green-safe behavior, orange-unsafe behavior).

TABLE I

INTRODUCTION OF FEATURES

Features	Details	
	Description	Source
Yaw_Mean	The mean of the yaw angle of the simulated vehicle	[a] DS
Yaw_Std	The degree of yaw angle deviating from the mean	DS
Wheel steering_Mean	The mean of wheel steering angle in the simulated vehicle	DS
Wheel steering_Std	The degree of steering angle deviating from the mean	DS
Pupil size_Mean	The average pupil size	Tobii Pro
Pupil_size_Std	Discreteness of pupil size variation	Tobii Pro
Eye movement_Mean	The average movement of pupils	Tobii Pro
Eye Movement_Std	The fluctuation range of pupil movement distance	Tobii Pro
Accelerometer	Raw data from a smartwatch's XYZ-axis accelerometer	Garmin
BBI	The interval between two heart beats	Garmin
Heart rate	The heart beating times per minute	Garmin
Road type	Urban road or mountain road	DS

[a]*DS: Driving simulator*

recorded in the driving simulator, where the mean and standard deviation within each time window were used as the features of vehicle information. Physiological data contained eye-tracker data (pupil size and pupil movement), heart rate, beat-to-beat interval (BBI, an important indicator in cardiology and physiology showing the time duration between two consecutive heartbeats), and accelerometer (ACC, the rate of change in velocity and acceleration of smartwatch along XYZ-axis to understand user's movement and physical activity). In addition, the road environment (urban road or mountain road) was regarded as an environmental feature.

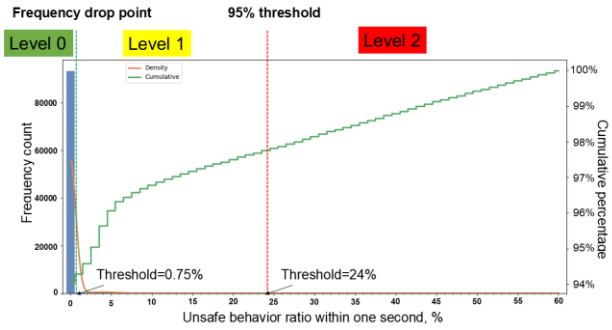

Fig 3. Frequency distribution histogram of the proportion of unsafe driving behavior within one second (green line-cumulative frequency distribution curve; orange line-distribution density curve; green dash line and red dash line indicated the thresholds.)

IV. RESULT AND DISCUSSION

A. *Classification of risk level*

As illustrated in Fig 3, the frequency distribution of unsafe driving behaviors proportion was plotted based on the classification method above. With the fitted distribution curve, the driving behaviors were naturally identified at the point where the variation of frequency density began to flatten (0.75%), and the 95th percentile threshold (24%) as the criteria for distinguishing among the three levels: Level 0, Level 1, and Level 2.

B. *Prediction window*

After multiple trials, the hyperparameters with values of LSTM were fixed as the model architecture of 3 layers, loss function of cross-entropy, batch size of 32, and epochs of 200. For prevention of overfitting, an early stop with patience of 10 was input. According to George et al.'s work, 30 seconds was a great period as time window to capture driver's variation of physiological index [14]. Also, a 30-second window size could avoid excessive computational burden with relatively complete time-series information. In order to evaluate the performance of LSTM model while various prediction scales were applied, the critical metrics (accuracy, precision, recall, and F1-score) were computed. Accuracy denotes the overall proportion of correctly predicted instances, while precision is defined as the ratio of truly positive instances among those

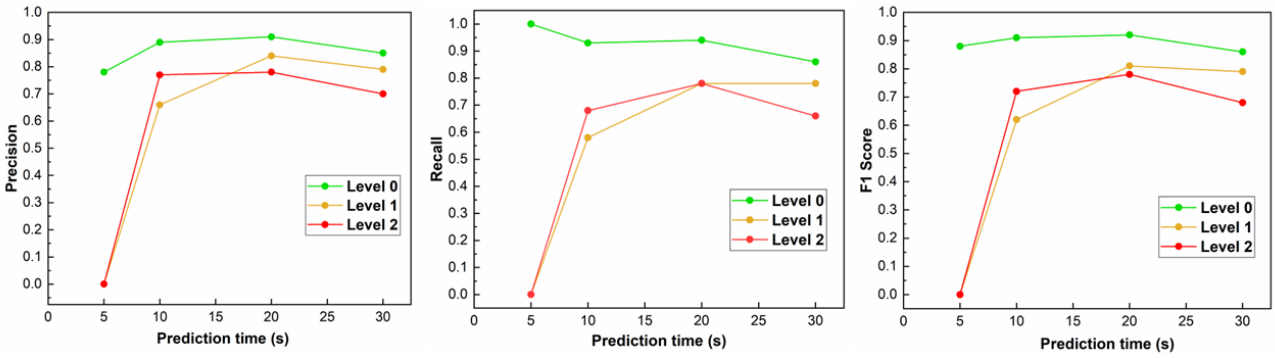

Fig 4. Comparison of the precision, recall, and F1-score of three safety levels at various prediction scales.

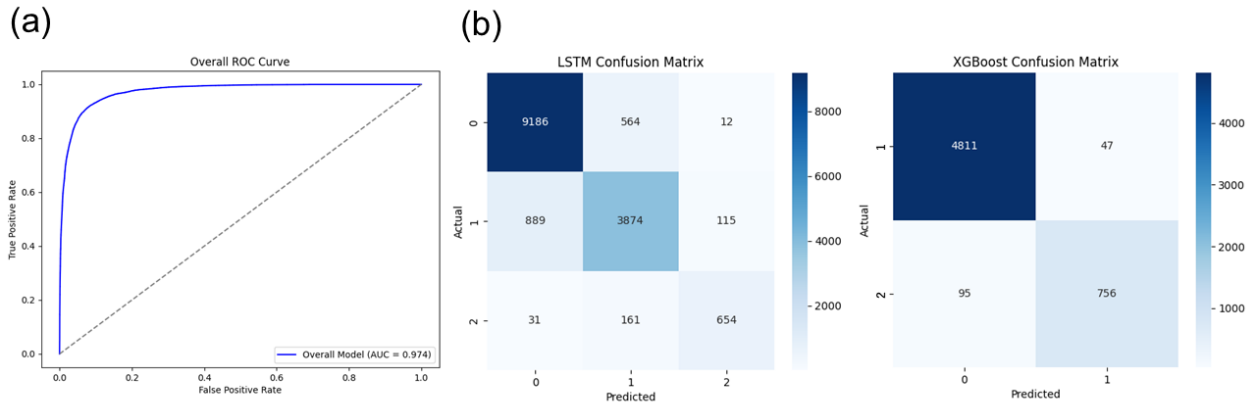

Fig 5. (a) The receiver operating characteristic curve (ROC) of the driving safety prediction using LSTM-XGBoost model. (b) The confusion matrix of prediction results using LSTM-attention and XGBoost fine-tuning, respectively.

TABLE II

RESULTS OF COMPARATIVE MODELS

Model	Performance			
	Accuracy	*Precision*	*Recall*	*F1-score*
LSTM	88.58%	86.28%	83.60%	84.88%
XGBoost	65.26%	52.55%	56.39%	53.49%
RF	62.76%	49.31%	53.98%	48.55%
SVM	56.51%	43.49%	47.01%	35.82%
This study	89.97%	90.53%	87.84%	89.15%

predicted as positive. Recall represents the fraction of true positive instances correctly identified by the model, and the F1-score, serving as a balanced measure, is the harmonic mean of precision and recall. The computational formulas are provided in Equations (11) to (14).

$$Accuracy = \frac{TP+TN}{TP+TN+FP+FN} \tag{11}$$

$$Precision = \frac{TP}{TP+FP} \tag{12}$$

$$Recall = \frac{TP}{TP+FN} \tag{13}$$

$$F1-Score = \frac{2\times Precision\times Recall}{Precision+Recall} \tag{14}$$

The global accuracy of LSTM models with various prediction scales of 5, 10, 20, and 30 seconds were obtained 68.69%, 83.66%, 87.86%, and 82.05%, respectively. From Fig 4, it can be observed that 5-second prediction window could hardly foresee category 'Level 1' and 'Level 2', due to a high instability over short periods. Conversely, the F1-score of a 30-second prediction window for category 'Level 2' of high risk decreased, indicating that a longer prediction window might introduce noise or dilute features. With the greatest F1- scores for both 'Level 1' and 'Level 2' when a 20-second prediction window was applied, the period of 20 seconds in prediction was selected as the optimized condition in LSTM.

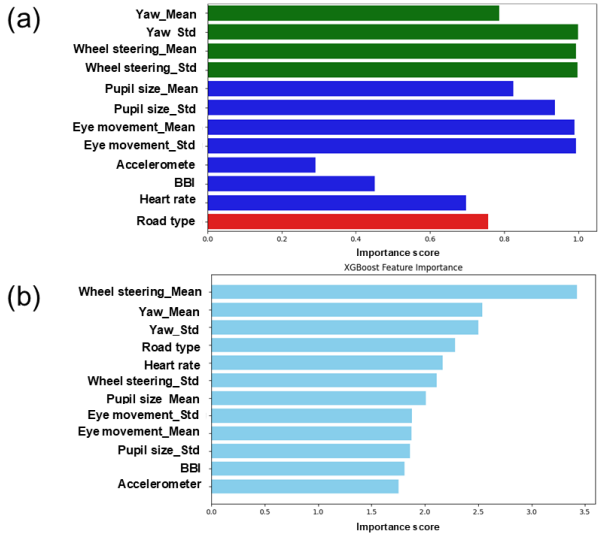

Fig 6. The importance of all the features: (a) LSTM-attention: the driving and vehicle features from DS are marked green, physiological features are marked blue, and environmental feature is marked red; (b) XGBoost: the feature importance ranking in the prediction of 'Level 1' and 'Level 2'.

C. *Evaluation of the performance*

According to grid search method, the optimized parameters of XGBoost were set as 'n-estimators=800', 'max depth=12', 'learning rate=0.02', 'subsample=0.71', and 'colsample bytree=0.69'. The proposed hybrid approach demonstrated capability for 20-second-ahead prediction of driver operational states. In Fig. 5(a), the model demonstrated ideal effectiveness of classifying different levels with area under the curve (AUC) of 0.974. For further validation, the implementations of LSTM, XGBoost, random forest (RF), and support vector machine (SVM) were systematically shown in Table II for comparison. From the comparative results, it was observed that all models exhibited optimal

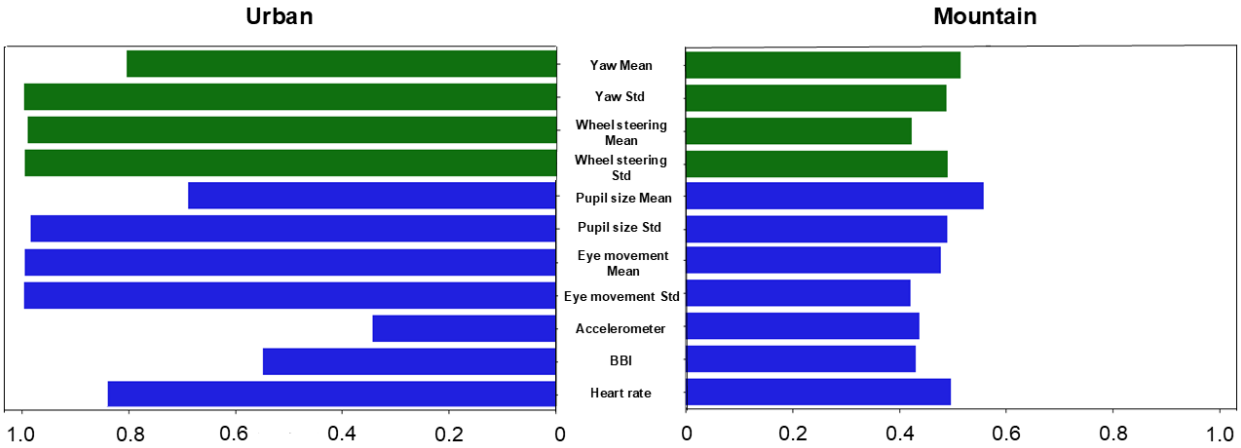

Fig 7. The feature importance on urban road and mountain road.

performance in predicting 'Level 0' events, attributable to the predominance of this category in the imbalanced dataset. However, the LSTM architecture significantly outperformed other models in minority-class predictions (Levels 1 and 2), stemming from the LSTM inherent capacity of capturing dependencies in time sequential behavioral data. When XGBoost was fine-tuned as a calibrator for minority-class outputs from LSTM-attention, the intact system achieved classification metrics (precision, recall, F1-score) exceeding 87% across all categories, demonstrating robustness to class imbalance. The confusion matrix of both LSTM-attention and XGBoost fine-tuning are shown in Fig. 5(b).

C. Evaluation of the feature importance

In attention mechanisms, importance scores (attention weights) are softmax-normalized values (summing to 1) that quantify the relative relevance of input elements, where higher scores indicate stronger focus on those features during processing. As visualized in Fig 6, features from driving simulator and eye state features shared equivalent importance, while that of the data collected by smartwatch were relatively lower. Among these features with LSTM (Fig, 6(a)), the yaw angle and steering wheel angle exhibited great importance in predicting hazardous driving behaviors. These parameters served as critical indicators of vehicular stability, with their dynamic variations directly correlating to loss of control probabilities [15][16]. Besides vehicular dynamics, pupillary features (eye movement and pupil size) also demonstrated considerable predictive relevance, as saccadic magnitude correlates with attentional allocation, while pupillary oscillations are physiologically linked to cognitive workload and stress responses [17][18]. In brief, reduced saccadic frequency reflects enhanced attentional focus, thereby decreasing reaction latency to unexpected events. Pupillometric analysis further indicates that oscillation frequency of pupillary constriction/dilation cycles exhibits positive covariance with cognitive processing demands, while marked pupillary instability reliably signals cognitive overload states. Cardiovascular measures concurrently contribute to behavioral prediction matrices. Previous studies have demonstrated that elevated heart rate is significantly associated with heightened stress levels and aggressive driving behaviors, which are recognized as critical contributors to unsafe driving practices and compromised road safety [19]. When predicting relatively unsafe driving behaviors, wheel steering and yaw angle played a more important role than physiological features, indicating that unsafe driving behaviors are more likely to occur when turning (Fig. 6(b)).

In order to investigate the importance of features in different scenarios, the comparison of the attention weights on urban and mountain roads were compared in Fig 7. In urban road scenarios, the significance of features closely aligned with the overall pattern in Fig 6. In contrast, on mountain roads, the attention weights assigned to individual features tended to be uniformly distributed, indicating that no single feature overwhelmingly dominated the model's decision-making process. Moreover, the overall feature importance derived from the attention mechanism was found to be lower in the mountainous scenario compared to the urban scenario due to the increased complexity and variability of mountain roads, where diverse features contributed equally to driving behavior, thereby diluting the influence of any single feature. These findings highlight the requirements for more robust or context-adaptive modeling strategies to effectively capture evident features in complex and dynamic driving environments such as mountain roads.

D. Potential application

The proposed model has demonstrated great performance in the domain of risk prediction, which holds significant implications for advancing in-cabin safety monitoring technologies. Based on our previous study in driving cognitive assessment, the methodology developed in this study effectively further addresses existing gaps in real-time driving safety evaluation. The capacity to provide real-time feedback to drivers will facilitate both risk reduction and

behavioral coaching. This implementation enables the integration of cognitive evaluation with driving risk analysis, thereby establishing a unique application.

V. Limitation

Although the hybrid model demonstrated a promising performance on the existing dataset, several limitations were identified in this study. Compared with naturalistic driving data, driving simulators exhibit constraints including reduced environmental complexity, limited sensory feedback, and attenuated risk prediction. On the other hand, the fixed scenarios and routes in driving simulators might introduce behavioral artifacts due to the influence of the participants' familiarity with the simulated environment. Moreover, incomplete datasets due to unexpected partial recording deficiencies prevented comprehensive model training using all available data. Hence, the effectiveness of this model for on-road driving tests remains to be verified through extended studies.

VI. Conclusion

This study developed a method that integrated multimodal driving experimental data, applied LSTM-attention to predict driving risks, and further used XGBoost for fine-tuning. The model demonstrated excellent performance when handling various feature values with AUC of 0.974. Compared to other approaches commonly used, this model addresses the data imbalance issue by fine-tuning the minority categories (Level 1 and Level 2) through XGBoost, without intervening in the feature weight values. Also, it has shown a superior performance in terms of precision, recall and F1-score, indicating the exceptional performance in balancing sensitivity and specificity. Moreover, the attention mechanism was introduced to reveal the distribution of importance among various features, enhancing the interpretability of the model. While driving on different types of roads, eye status features strongly correlated to driving safety prediction, especially on urban roads. In future work, we plan to apply this model to naturalistic driving experiments to validate its effectiveness in real-world driving scenarios and explore how to predict driving behavior over a period of longer time.

References

[1] World Health Organization, "Global status report on road safety 2018," in Public Health Policy, 3rd ed. vol. 5, J. Peters, Ed. Geneva: World Health Organization, 2018, pp. 1–256.

[2] D. L. Hendricks, M. Freedman, and J. C. Fell, "The relative frequency of unsafe driving acts in serious traffic crashes," U.S. Department of Transportation, Washington, DC, Tech. Rep. DOT-HS-809-206, 2001.

[3] M. E. Rakauskas, N. J. Ward, E. R. Boer, E. M. Bernat, M. Cadwallader, and C. J. Patrick, "Combined effects of alcohol and distraction on driving performance," Accid. Anal. Prev., vol. 40, no. 5, pp. 1742–1749, 2008.

[4] R. Vivoli, M. Bergomi, S. Rovesti, P. Bussetti, and G. M. Guaitoli, "Biological and behavioral factors affecting driving safety," J. Prev. Med. Hyg., vol. 47, no. 2, pp. 69–73, 2006.

[5] P. M. Salmon, G. J. Read, V. Beanland, J. Thompson, A. J. Filtness, A. Hulme, and I. Johnston, "Bad behaviour or societal failure? Perceptions of the factors contributing to drivers' engagement in the fatal five driving behaviours," Appl. Ergon., vol. 74, pp. 162–171, 2019.

[6] T. H. Weisswange, B. Bolder, J. Fritsch, S. Hasler, and C. Goerick, "An integrated ADAS for assessing risky situations in urban driving," in Proc. IEEE Intell. Veh. Symp., Gold Coast, Australia, 2013, pp. 292–297.

[7] S. Mozaffari, O. Y. Al-Jarrah, M. Dianati, P. Jennings, and A. Mouzakitis, "Deep learning-based vehicle behavior prediction for autonomous driving applications: A review," IEEE Trans. Intell. Transp. Syst., vol. 23, no. 1, pp. 33–47, 2020.

[8] C. Bai, S. Jin, J. Jing, C. Yang, W. Yao, D. Rong, and J. A. Alagbé, "A multimodal data-driven approach for driving risk assessment," Transp. Res. E, vol. 189, Art. 103678, 2024.

[9] S. M. Lavrenz, E. I. Vlahogianni, K. Gkritza, and Y. Ke, "Time series modeling in traffic safety research," Accid. Anal. Prev., vol. 117, pp. 368–380, 2018.

[10] R. Zhang, X. Wen, H. Cao, P. Cui, H. Chai, R. Hu, and R. Yu, "Critical safety management driver identification based upon temporal variation characteristics of driving behavior," Accid. Anal. Prev., vol. 193, Art. 107307, 2023.

[11] L. Eboli, G. Mazzulla, and G. Pungillo, "Combining speed and acceleration to define car users' safe or unsafe driving behaviour," Transp. Res. C, vol. 68, pp. 113–125, 2016.

[12] Y. Wang, J. Zhang, and G. Lu, "Influence of driving behaviors on the stability in car following," IEEE Trans. Intell. Transp. Syst., vol. 20, no. 3, pp. 1081–1098, 2018.

[13] J. Boylan, D. Meyer, and W. S. Chen, "A systematic review of the use of in-vehicle telematics in monitoring driving behaviours," Accid. Anal. Prev., vol. 199, Art. 107519, 2024.

[14] G. Panagopoulos, "Forecasting markers of habitual driving behaviors associated with crash risk," IEEE Trans. Intell. Transp. Syst., vol. 21, no. 8, pp. 3187–3196, 2020.

[15] J. Ackermann, "Safer car driving by robust steering control," in Proc. UKACC Int. Conf. Control, Exeter, UK, 1996, p. 733.

[16] H. Du, N. Zhang, and G. Dong, "Stabilizing vehicle lateral dynamics with considerations of parameter uncertainties and control saturation through robust yaw control," IEEE Trans. Veh. Technol., vol. 59, no. 5, pp. 2593–2597, 2010.

[17] Z. Bian, R. Pierce, and G. Andersen, "Eye movement patterns and driving performance," in Proc. 6th Int. Driv. Symp. Hum. Factors, Lake Tahoe, CA, 2011, pp. 1–8.

[18] S. M. Usman, A. J. Khattak, S. Chakraborty, I. Mahdinia, and R. Tavassoli, "Detection of distracted driving through the analysis of real-time driver, vehicle, and roadway volatilities," J. Transp. Saf. Security, vol. 16, no. 7, pp. 880–901, 2024.

[19] J. E. Meseguer, C. T. Calafate, and J. C. Cano, "On the correlation between heart rate and driving style in real driving scenarios," Mob. Netw. Appl., vol. 23, no. 1, pp. 128–135, 2018.